Bažant, Z.P. (1990), "Rate effect, size effect and non-local concepts for fracture of concrete and other quasi-brittle materials." Preprints, *NATO Advanced Research Workshop* on "Toughening Mechanisms in Quasi-Brittle Materials, Northwestern University, S. P. Shah, ed., 143–166.

Toughening Mechanisms in Quasi-Brittle Materials

edited by

S. P. Shah

NSF Science and Technology Center for Advanced Cement-Based Materials,
Robert R. McCormick School of Engineering and Applied Sciences,
Northwestern University, Evanston, Illinois, U.S.A.

Kluwer Academic Publishers

Dordrecht / Boston / London

Published in cooperation with NATO Scientific Affairs Division

RATE EFFECT, SIZE EFFECT AND NONLOCAL CONCEPTS FOR FRACTURE OF CONCRETE AND OTHER QUASI-BRITTLE MATERIALS

Zdeněk P. Bažant
Walter P. Murphy Professor of Civil Engineering
Northwestern University, Evanston, Illinois 60208, USA

ABSTRACT. The lecture reviews several recent results achieved at Northwestern University in the problem of size effects and nonlocal concepts for concrete and other brittle heterogeneous materials, and presents a new method for calculating the load-deflection curves of fracture specimens or structures with time-dependent crack growth and viscoelastic material behavior. The results reviewed deal with the size effect law in fracture and its exploitation for determining material fracture characteristics, statistical generalization of the size effect law with a nonlinear reformulation of Weibull's weakest-link theory, determination of the size dependence of the fracture energy determined by work-of-fracture method, nonlocal models for smeared cracking and damage, microstructural determination of the nonlocal material properties and fracture process zone behavior, size effect in fatigue fracture of concrete, and use of the size effect for determining the fracture properties of high-strength concrete.

1. Introduction

Fracture analysis of concrete structures has to deal with two important complicating characteristics: the distributive nature of cracking and damage in concrete, which causes the fracture process zone to be relatively large and engenders a size effect, and time dependence of both the crack growth and the material behavior. The nonlinear behavior caused by the existence of a large fracture process zone has been in the focus of attention for some time and its treatment is becoming quite well understood [1-3, etc.]. Attention to the size effect is more recent [8] but it has already led to some useful extensions of fracture theory and a new method for determining material fracture properties [4-7, 9-12]. The existence of the rate effect has been known for a long time and has been studied extensively with regard to dynamic fracture. However, the nonlinear fracture aspects of the rate effect, which are manifested in interaction with the size effect, have not received attention until recently, although they are no doubt very important for predicting the response of structures.

The present lecture intends: (1) to present a new effective and relatively simple method for calculating the load-deflection response of a structure with a large fracture process zone, time-dependent fracture growth, and viscoelastic material properties; and (2) to review several recent results achieved at Northwestern University. No claims for exhaustive or even balanced coverage of the latest developments are made. Due to exploding research

S. P. Shah (ed.), Toughening Mechanisms in Quasi-Brittle Materials, 131–153.

activity, this would be beyond the scope of the present paper.

2. Review of Some Recent Results

2.1 A REVIEW OF SIZE-EFFECT - THE SALIENT CHARACTERISTIC OF FRACTURE

The structural size-effect is the most important characteristic and the easiest measurable consequence of nonlinear fracture behavior. Considerable attention has been devoted at Northwestern University to the phenomenologic description of the size effect [8-12] as well as its physical mechanism. We will begin by a brief overview of the latest phenomenologic characterization of fracture in terms of the size effect and the consequences for the measurement of fracture properties.

The size effect may be defined in terms of the nominal strength $\sigma_N = c_n P_u/bd$ (for 2D) or $c_n P_u/d^2$ (for 3D) in which P_u = maximum load of geometrically similar specimens of size d (dimension) and, in case of two dimensions, thickness b; c_n = factor chosen for convenience. Under the assumption that there is a large fracture process zone that is not negligible compared to d, and that the crack at failure of geometrically similar structures of different sizes is also geometrically similar, the nominal strength approximately obeys the size effect law [8]:

$$\sigma_N = B f_u (1+\beta)^{-1/2}, \qquad \beta = d/d_0 \tag{1}$$

in which f_u = any measure of material strength, e.g., the tensile strength, and B, d_0 = empirical constants. This law describes a smooth transition from plastic limit analysis, for which there is no size effect (σ_N = constant) to linear elastic fracture mechanics (LEFM), for which the size effect is the maximum possible, given by $\sigma_N \propto \beta^{-1/2}$. The plot of Eq.1 is shown in Fig.1. The horizontal asymptote represents the limiting case of plastic limit analysis, and the inclined asymptote of slope - 1/2 the limiting case of LEFM. Parameter d_0, called the transitional size, corresponds to the intersection of these two asymptotes. Eq.1 has originally been derived by dimensional analysis and similitude arguments, based on the hypothesis that the energy release due to fracture depends not only on the fracture length but also on a second length characteristic that is approximately a material property and characterizes either the effective length or the effective width of the fracture process zone, or the nonlocal properties of an equivalent continuum.

Under certain further simplifying assumptions based on equivalent LEFM, it has been shown [11] that the size effect law from Eq.1 can also be written in the form

$$\sigma_N = c_n \left(\frac{E G_f}{g'(\alpha_0) c_f + g(\alpha_0) d} \right)^{1/2} \tag{2}$$

in which G_f = fracture energy of the material, defined as the energy required for crack propagation in an infinitely large specimen, E = Young's elastic modulus, c_f = effective length of the fracture process zone in an infinitely large specimen (a material constant), $\alpha_0 = a_0/d$, a_0 = length of initial notch of crack, and $g(\alpha)$ = non-dimensionalized energy release rate of the specimen of the given geometry, which is obtained by writing the LEFM solution

for the energy release rate in the form $G = P^2 g(\alpha)/E\, b^2\, d$ where P is the applied load or reaction, $\alpha = a/d$, $a = a_0 + c$, c = crack extension from the notch or initial crack tip. These formulas are valid for plain stress. For plain strain or axisymetric propagation, E must be replaced by $E/(1-\nu^2)$. Defining the so-called intrinsic strength $\tau_N = (P_u/bd)g'(\alpha_0)$ and intrinsic size $\bar{d} = g(\alpha_0)d/g'(\alpha_0)$, one can rewrite Eq.2 in the form

$$\tau_N = \left(\frac{E\, G_f}{c_f + \bar{d}}\right)^{1/2} \tag{3}$$

which involves only material constants EG_f and c_f. Comparing Eq.2 or 3 with Eq.1, one gets the following expressions for material fracture constants

$$G_f = \frac{B^2 f_u^2}{c_n^2 E} d_0 g(\alpha_0), \quad c_f = d_0 \frac{g(\alpha_0)}{g'(\alpha_0)} \tag{4}$$

Thus, after measuring the maximum loads for geometrically similar specimens of sufficiently different sizes, one can determine B and d_0 by least-square fitting all the data (Eq.1 can be rearranged to a linear regression plot), and then evaluate the fracture energy and the effective process zone length from Eq.4 (strictly on the basis of maximum load data). This method is probably the easiest to implement in the laboratory (even a soft testing machine is adequate and no measurements of displacements or crack lengths are required). The method has been verified by numerous tests on concrete and rock. The results are, by definition, size independent and they were also proven to be approximately shape independent, since very different fracture specimen geometries furnished approximately the same results, as expected theoretically.

The ratio β, which may be calculated by one of the following two expressions,

$$\beta = \frac{g(\alpha_0)}{g'(\alpha_0)} \frac{d}{c_f}, \qquad \beta = \frac{B^2 g(\alpha_0)}{c_n^2} \frac{d\, f_u^2}{E\, G_f} \tag{5}$$

is called the brittleness number. For $\beta \to 0$, plasticity applies, and for $\beta \to \infty$, LEFM applies. For $\beta < 0.1$ it is possible to use plasticity as an approximation, and for $\beta > 10$ it is possible to use LEFM. For the intermediate β-values, nonlinear fracture mechanics must be used. However, if the transitional size d_0 is determined, an approximate prediction of maximum load can be obtained by interpolating between the solutions of plasticity and LEFM according to Eq.1. This should be useful for design; proposals to modify the existing design formulas for diagonal shear failure of beams (without or with stirrups, unprestressed or prestressed), punching shear failure of slabs, torsional failure of beams, pullout failures of bars and of studded anchors have been made and verified by extensive tests [14-22].

Based on size effect measurements, other basic nonlinear fracture characteristics can also be obtained. The critical crack-tip opening displacement may be determined as

$$\delta_c = \frac{8\, K_{If}}{E} \sqrt{\frac{c_f}{2\pi}}, \qquad \text{with} \quad K_{If} = \sqrt{E\, G_f} \tag{6}$$

Furthermore, the R-curve (resistance curve) for the specimen or structure can be calculated as

$$R(c) = G_f \frac{g'(\alpha_1)}{g'(\alpha_0)} \frac{c}{c_f}, \quad \text{with} \quad \frac{c}{c_f} = \frac{g'(\alpha_0)}{g(\alpha_0)} \left(\frac{g(\alpha_1)}{g'(\alpha_1)} - \alpha_1 + \alpha_0 \right) \tag{7}$$

in which α_1 is a dummy parameter representing the relative crack length for the structure size for which $R(c)$ corresponds to the maximum load (Fig.2). Choosing various values of α_1, the values of R (critical G-value required for further crack growth) and c can be calculated from Eq.7, and thus the $R(c)$-curve defined parametrically. This curve is by definition size independent but depends on the geometry of the structure. For very different geometries, very different R-curves can be obtained. Eq.7 defines the master R-curve for an infinitely large specimen. For a specimen of finite size, the R-curve given by Eq.7 is followed only up to the maximum load P_u, and after that the actual R-curve is constant (horizontal), with the R-value equal to that attained at the peak load [23, 24]. The reason is that for prepeak loading the fracture process zone grows in size while remaining attached to the crack or notch tip (provided structures with $g'(\alpha_0) > 0$ are considered), whereas in post-peak softening the fracture process zone gets detached from the notch tip and travels ahead retaining approximately a constant size.

Using the equivalent LEFM approach, the curve of load or reaction P versus the load-point displacement u may be calculated from the equations

$$u = P \left(C_0 + \frac{2}{bE} \int_0^{\alpha} g(\alpha') d\alpha' \right), \qquad P = b \sqrt{\frac{Ed}{g(\alpha)} R(c)} \tag{8}$$

in which C_0 is the compliance for a specimen without any crack. Choosing various values of c, with $\alpha = (a_0 + c)/d$, the values of P and u can be evaluated from Eq.8, defining the load-deflection curve parametrically.

Eq.8 provided a strong verification of the size effect method of determining fracture properties. The material fracture parameters were determined solely from the maximum loads measured on geometrically similar rock fracture specimens of very different sizes [23]; then the R-curve was calculated from Eq.7, and from that the load-deflection diagram shown in Fig.3 from Eq.8 was computed. The results showed excellent agreement with the measured load deflection curve (Fig.3). Similar agreement has been obtained for concrete [13].

2.2. STATISTICAL GENERALIZATION AND WEIBULL'S EFFECT

The fact that Eq.1 or Eq.3 can be algebraically rearranged to a linear regression plot of $Y = \tau_N^{-2}$ versus $X = \bar{d}$ makes it possible to obtain easily the statistics of the material fracture parameters. The coefficients of variation of fracture toughness (defined for a specimen of infinite size), the effective length of the fracture process zone, and the fracture energy may be approximately obtained as

$$\omega_{K_{If}} = \frac{1}{2}\omega_A, \quad \omega_{c_f} = (\omega_A^2 = \omega_c^2)^{1/2}, \quad \omega_{G_f} = (4\omega_{K_{If}}^2 + \omega_E^2)^{1/2} \tag{9}$$

in which ω_A and ω_C are the coefficients of variation of the aforementioned slope and of the

Y-intercept of the linear regression plot, and ω_E is the coefficient of variation of the elastic modulus of concrete [11].

Eq.9 takes care only of the uncertainty of the material parameter values in the foregoing deterministic model. More realistically, one should note that the failure process in itself is stochastic, and the simplest vehicle to take that into account is Weibull's reasoning. However, the classical Weibull-type formulations do not apply to concrete structures because they exhibit stable growth of cracking with significant stress redistributions prior to maximum load. Good results, however, can be obtained with a nonlocal generalization of Weibull approach [25], in which the survival probability of the structure is calculated as the joint probability of survival of all the material elements based on the stress distribution just prior to failure, in which the material failure probability is determined from Weibull distribution using the nonlocal stress average, $\bar{\sigma}_i$;

$$-\ln(1-P_f)=\int_V \sum_{i=1}^{n}\left(\frac{\bar{\sigma}_i}{\sigma_0}\right)^m \cdot \frac{dV}{V_0}, \quad \bar{\sigma}_i(x)=\int_V \alpha(\mathrm{s}-\mathrm{x})\sigma_i(\mathrm{s})dV(s) \tag{10}$$

in which P_f = failure probability of the structure, σ_i = principal stresses ($i = 1,2,3$), V = volume of the structure, V_0 = volume of a small representative volume of the material, x,s = coordinate vectors, $\alpha(\mathrm{s}-\mathrm{x})$ = given weighting function of a nonlocal material model (based on characteristic length ℓ); and m, σ_0 = Weibull modulus and scale parameter determined by fitting Weibull distribution to direct tensile test data (assuming a zero Weibull threshold). It has recently been found [25] that the nonlocal Weibull concept leads, under certain approximations, to the following generalization of the size effect law (Fig.4).

$$\bar{\sigma}_N = B f_u(\beta^{2n/m}+\beta)^{-1/2} \tag{11}$$

in which the overbar denotes the mean nominal strength, $\bar{\sigma}_N$; and $n = 2$ or 3 for two- or three-dimensional similarity. For concrete, typically $m = 12$. For large structure sizes, Eq.11 aproaches LEFM, same as Eq.1. For small structure sizes, $\beta \to 0$, Eq.11 asyptotically approaches the classical Weibull size effect, $\bar{\sigma}_N = \beta^{-n/m}$, which gives a rather weak size effect, $\bar{\sigma}_N = \beta^{-1/6}$ for two-dimensional similarity. Thus, Eq.11 represents a smooth transition from the classical Weibull size effect to LEFM. Eq.11 has been shown to agree with the data for concrete somewhat better than Eq.1, but the difference is rather small except when dealing with very small structure sizes. The formulation in Eq.2-7 can be generalized in accordance with Eq.11.

2.3. SIZE DEPENDENCE OF FRACTURE ENERGY OBTAINED BY CURRENT RILEM METHOD

The fact that the size effect method based on the maximum load yields excellent predictions of the load-deflection curves, in good agreement with measurements, makes it possible to exploit this formulation for examining the fracture energy determined from the area under the load-deflection curve, which represents the work-of-fracture method proposed for ceramics by Nakayama [26], and by Tattersall and Tappin [27], and introduced for concrete by [28,29]. The work of fracture has been calculated for concrete specimens on the basis

of the load-deflection curve obtained from the R-curve (Eqs.7 and 8), keeping the R-value constant for the post-peak softening (area in Fig.2c). This calculation indicates a size effect on the value of the fracture energy G_f^R, due to the fact that the peak load occurs at different points of the R-curve for specimens of different sizes. The calculation results are shown in Fig.2d; note that the size dependence of G_f^R is quite strong, in fact stronger than that of the R-curve, although not as strong as that of the apparent fracture energy G_c determined by LEFM method. This agrees with the conclusions of Planas and Elices [4], who showed that the fracture energy measurements according to the RILEM standard, which is based on the work-of- fracture method, must be extrapolated to a specimen of infinite size in order to obtain consistent (size independent) results.

2.4. NONLOCAL DAMAGE MODELS

In finite element analysis of damage and cracking in concrete structures, the size effect has long been neglected. Unfortunately, most of the existing models are based on plasticity or its modifications and exhibit no size effect, which is unacceptable for concrete structures. Modeling of the size effect should be accepted as the basic criterion for correctness of a finite element code. The only way to achieve a correct size effect in agreement with Eq.1 is to either use some type of a nonlinear fracture model for a line crack with cohesive crack-bridging zone, or a nonlocal form of a finite element code for distributed damage of smeared cracking. The latter approach is more versatile and perhaps somewhat more realistic due to the diffuse nature of cracking in reinforced concrete structures. A nonlocal generalization of the classical smeared cracking formulation has been introduced in [30], and a good agreement with size effect data and with Eq.1 has been demonstrated. A more realistic constitutive flaw for the evolution of damage or cracking in the fracture process zone is the microplane model, in which the material properties are characterized separately on planes of various orientation in the material. This model has recently been generalized to a nonlocal form, and it was again demonstrated that such a generalization agrees well with size effect fracture data as well as Eq.1 (Fig.5); see [31].

2.5. MICROMECHANICS MODELING

It is very difficult to identify the strain-softening constitutive relations for the fracture process zone on the basis of measurements alone. Therefore, micromechanics modeling could be of great help. Micromechanics models need to represent systems of microcracks that are observed experimentally. Therefore, initial studies of micromechanics of fracture of concrete concentrated on the analysis of an array of cracks in a homogeneous elastic matrix. Some observed features could be reproduced with such models, particularly the strain-softening behavior. This was, for example, demonstrated for an array of parallel microcracks spaced on a cubic lattice and subjected to a microscopic uniaxial stress field. Application of the homogenization conditions to such a crack array also showed that the corresponding macroscopic smoothing continuum is nonlocal, and of the nonlocal damage type. Stability analysis of the interacting crack systems, however, indicated that such a model is unrealistic because only one of the cracks can grow in a stable manner, which is of course not what is seen in

experiments. The reason for this discrepancy no doubt consists in the micro-inhomogeneity of the material, especially the presence of harder inclusions.

Interaction of cracks and inclusions in an elastic matrix has been studied in [32], using a Green's function approach (Fig.6). Approximate solutions have been obtained for a crack interacting with many inclusions, for various geometric configurations. The solution was used to obtain an apparent R-curve of a microcrack in a smoothed homogeneous matrix such that its growth is the same as the growth of the actual crack interacting with inclusions. It was found that in many situations the apparent R-curve is rising, which has a stabilizing effect on the system of cracks. The apparent rising R-curve can stabilize a system of many cracks, such that many cracks can grow simultaneously, in agreement with observations.

As a conclusion from this study, it appears that a study of crack arrays in a homogenous continuum is in general insufficient, and the presence of inhomogeneities representing the aggregate pieces must be considered simultaneously in the analysis. It should be also noted that this result is similar to that of Gao and Rice [33], who used perturbation method; however, they considered only the case when the elastic moduli of matrix and inclusions differ very little. A special problem of this type has also been solved by Mori et al. [34].

2.6. SIZE EFFECT CORRECTION TO PARIS LAW FOR FATIGUE FRACTURE

Under repeated loading, cracks tend to grow, which is described by the well-known Paris law [35, 36]. Applicability of this law to fatigue crack growth in concrete has been verified by Swartz et al. [37]. Since Paris law describes the crack growth as a function of the amplitude of the stress intensity factor, a question arises with respect to the size effect. In monotonic loading, the stress intensity factor does not provide sufficient characterization of fracture when different sizes are considered, as is known from the previously discussed size effect law. The same phenomenon must be expected for cyclic fracture, especially since fracture under monotonic loading can be regarded as a limiting case of fracture under cyclic loading. Recent fatigue fracture experiments on notched concrete beams at Northwestern University [38] have shown that the fatigue crack growth in geometrically similar specimens of different sizes can be described by the following law:

$$\frac{\Delta a}{\Delta N} = C\left(\frac{\Delta K_I}{K_{I_c}}\right)^n, \qquad K_{I_c} = K_{I_f}\left(\frac{\beta}{1+\beta}\right)^{1/2} \tag{12}$$

in which K_{I_f} = fracture toughness for an infinitely large specimen, ΔK_I = amplitude of the stress intensity factor, K_{I_c} = apparent fracture toughness derived from Eq. 1; $\Delta a/\Delta N$ = crack length extension per cycle; and C, n = constants. For $\beta \to \infty$, this equation reduces to the well-known Paris law. For normal size concrete specimens, however, the deviations from Paris law are quite significant. This is revealed by the experimental results in Fig.7 for three different sizes in the ratio 1:2:4. In this plot, the Paris law gives one inclined straight line of slope n for all sizes, but it is seen from Fig.7 that for each size the test results allign

on different straight line for each size. The three solid straight lines represent Eq.12.

2.7. FRACTURE OF HIGH STRENGTH CONCRETE

It has already been well established that high strength concrete is more brittle than normal strength concrete. This question has been investigated at Northwestern University using the size effect method of determining material fracture properties [13]. Concrete of 28-day standard compression strength 12,000 psi, typical for high-rise construction in the Chicago area, has been used.

The results are summarized in Fig.8, which shows the relative values of various material properties compared to the normal strength concrete, particularly the compression strength f'_c, modulus of rupture f_r, Young's modulus E, fracture toughness K_{I_c} and fracture energy G_f (both for an infinitely large specimen), effective length of the fracture process zone c_f, and Irwin's characteristic size of the nonlinear zone ℓ_0. Whereas the compression strength is 2.6-times higher than that of normal-strength concrete, the fracture toughness is increased only by about 25%, fracture energy by about 15%, and the effective lengths of the fracture process zone is decreased 2.5 times and the characteristic size of the nonlinear zone is *decreased* approximately 5-times.

Consequently, the brittleness number of the high strength concrete structure is approximately 2.5-times *higher* than the brittleness of an identical structure made of normal-strength concrete. This aspect of high strength concrete is unfavorable for design and requires special attention.

3. Effect of Rate of Loading and Creep

Fracture of rocks as well as ceramics is known to exhibit a significant sensitivity to the rate of loading. For concrete, the influence of the rate of loading on fracture propagation is even more pronounced and is further compounded by viscoelasticity of the material in the entire structure. To calculate the response of a structure, as well as to be able to evaluate laboratory measurements, the most important is the determination of the load or reaction P as a function of the load-point displacement u and time t for a prescribed loading regime. The following simple method has been formulated for this purpose.

We begin by rewriting Eq.8 for a structure with rate-independent fracture as follows

$$u = \frac{P}{E}\bar{C}(a), \quad \bar{C}(a) = \bar{C}_0 + \frac{2}{b}\phi(\alpha), \quad \phi(\alpha) = \int_0^{\alpha} [k(\alpha')]^2 d\alpha' \tag{13}$$

in which $\bar{C}(a)$ is the secant compliance of the structure at crack length a calculated for a unit value of Young's modulus ($E' = 1$) and the actual Poisson ratio ν; $\bar{C}_0$ is the elastic compliance of the same structure with $E' = 1$ with no crack; $\alpha = a/d$; $[k(\alpha)]^2 = b^2 g(\alpha)$; function $k(\alpha)$ is defined by writing the known solution of the stress intensity factor in the form $K_I = P\, k(\alpha)/b\sqrt{d}$. Eq. 13 is valid for plane stress conditions.

For plane strain conditions, E needs to be replaced by $E/(1-\nu^2)$; this replacement needs to be carried out in all the subsequent analysis.

Outside the fracture processs zone, concrete behaves as a linearly viscoelastic (aging)

material described, for uniaxial stress, by the stress-strain relation

$$\varepsilon(t) = \int_{t_0}^{t} J(t,t')d\sigma(t') \quad \text{(Stieltjes integral)} \tag{14}$$

provided that there is no shrinkage and thermal expansion or that they have a negligible effect; σ, ε = uniaxial stress and strain, $J(t,t')$ = given compliance function of the material that characterizes creep, representing strain at age t caused by a unit uniaxial stress applied at age t'. Eq. 14 may be written in an operator form as $\varepsilon(t) = \underline{E}^{-1}\sigma(t)$ where $\underline{E}^{-1}$ is the creep operator defined by Eq. 14.

The load-displacement relation for a structure exhibiting creep may be obtained from the corresponding elastic relation by replacing $1/E$ with the corresponding creep operation $\underline{E}^{-1}$. Doing this in Eq. 13, one gets

$$u(t) = \int_{t_0}^{t} J(t,t')d\{P(t')\bar{C}[a(t')]\} \tag{15}$$

The solution needs to be carried out numerically. To this end, time t is subdivided by discrete times $t_r (r = 0, 1, 2, 3 \ldots)$ into time steps $\Delta t_r = t_r - t_{r-1}$. Time t_0 represents the age at the first loading. Using the trapezoidal rule (the error of which is proportional to Δt^2), we may approximate Eq. 15 as

$$u_r = \sum_{s=1}^{r} J_{r,s-\frac{1}{2}}(P_s\bar{C}_s - P_{s-1}\bar{C}_{s-1}) \tag{16}$$

where subscript r refers to time t_r and $s - \frac{1}{2}$ refers to time $t_s - \Delta t_s/2$; $P_s = P(t_s); \bar{C}_s = \bar{C}[a(t_s)]; J_{r,s-\frac{1}{2}} = J(t_r, t_{s-\frac{1}{2}})$; and the initial load value is $P(t_0) = P_0 = 0$. Writing Eq. 16 for t_{r-1} instead of t_r, i.e.,

$$u_{r-1} = \sum_{s=1}^{r-1} J_{r-1,s-\frac{1}{2}}(P_s\bar{C}_s - P_{s-1}\bar{C}_{s-1}) \tag{17}$$

and subtracting this from Eq. 16 one gets

$$\Delta u_r = \frac{1}{E''_r}(P_r\bar{C}_r - P_{r-1}\bar{C}_{r-1}) + \Delta u''_r \tag{18}$$

in which $\Delta u_r = u_r - u_{r-1}$, $1/E''_r = J_{r,r-\frac{1}{2}}$ and

$$\Delta u''_r = \sum_{s=1}^{r-1}(J_{r,s-\frac{1}{2}} - J_{r-1,s-\frac{1}{2}})(P_s\bar{C}_s - P_{s-1}\bar{C}_{s-1}) \quad \text{for } r > 2 \tag{19}$$

(Bažant, ed., 1988, p. 116). The accuracy, however, is somewhat improved if, instead of $J_{r,r-\frac{1}{2}}$, the effective modulus approximation

$$1/E''_r = J_{r,r-1} = J(t_r, t_{r-1}) \tag{20}$$

is used for the last step. Eq. 19 is applicable only for $r \geq 3$. For the first two steps, the approximations of Eq. 15 are

$$\begin{aligned} &\text{for } r = 1: \quad \Delta u_1 = u_1 = J_{1,0} P_1 \bar{C}_1 \\ &\text{for } r = 2: \quad \Delta u_2 = J_{2,1}(P_2 \bar{C}_2 - P_1 \bar{C}_1) + (J_{2,\frac{1}{2}} - J_{1,\frac{1}{2}}) P_1 \bar{C}_1 \end{aligned} \tag{21}$$

The foregoing analysis must be supplemented by a law for the growth of crack length $a(t)$. Materials that under a constant very fast loading rate follow linear elastic fracture mechanics exhibit, at slower rates, crack growth that approximately obeys the law

$$\dot{a} = \kappa_c \left(\frac{K_I(P)}{K_{If}} \right)^n \exp\left[-\frac{U}{R_0} \left(\frac{1}{T} - \frac{1}{T_0} \right) \right] \tag{22}$$

in which K_I = stress intensity factor, U = activation energy of crack growth, R_0 = gas constant, T = absolute temperature, T_0 = reference temperature, and κ_c, n = empirical material constants. The applicability of this well-known relation to concrete has been verified in [39]. However, to take into account nonlinear fracture properties and obtain the correct transitional size effect (agreeing with the size effect law), Eq. 22 must be generalized as:

$$\dot{a} = \kappa_c \left(\frac{K_I(P)}{K_I^R(c)} \right)^n \exp\left[-\frac{U}{R_0} \left(\frac{1}{T} - \frac{1}{T_0} \right) \right] = f(P, a), \quad \text{with } K_I(P) = \frac{P k(\alpha)}{b\sqrt{d}} \tag{23}$$

where f is a function of P and a, as defined by this equation, and $K_I^R(c)$ is the given R-curve (determined in advance for the given structure geometry). For the time step t_{r-1}, t_r), Eq. 23 yields

$$\Delta a_r = f(P_{r-\frac{1}{2}}, a_{r-\frac{1}{2}}) \Delta t_r \tag{24}$$

The following algorithm may now be used in every time step Δt_r (for $r > 2$), in which the previous values $a_0, a_1, \ldots a_{r-1}; P_0, \ldots P_{r-1}, u_0, \ldots u_{r-1}$ are already known.

1. Setting $P_{r-\frac{1}{2}} = P_{r-1}$ and $a_{r-\frac{1}{2}} = a_{r-1}$, calculate $\Delta a_r = f(P_{r-a}, a_{r-1}) \Delta t_r$ (Eq. 24) as the first estimate, and set $a_{r-\frac{1}{2}} = a_{r-1} + \frac{1}{2}\Delta a_r, a_r = a_{r-1} + \Delta a_r$. Evaluate $\bar{C}_r = \bar{C}(a_r)$ from Eq. 13.

2. Loop on iterations.

3. Calculate $\Delta u_r''$ from Eq. 19. Then, using prescribed Δu_r (or prescribed P_r), calculate P_r (or Δu_r) from Eq. 18. Then calculate Δa_r from Eq. 24 and obtain updated values $a_{r-\frac{1}{2}} = a_{r-1} + \frac{1}{2}\Delta a_r$ and $a_r = a_{r-1} + \Delta a_r$. Evaluate updated $\bar{C}_r = \bar{C}(a_r)$ from Eq. 13.

4. Check the given tolerance citerion, requiring that the absolute value of the change of P_r in the last iteration be less than $|eP_r|$ where e is a given small number (e.g., $e = 10^{-6}$). If violated, go to 2 and start the next iteration. If satisfied, go to 1 and start the first iteration of the next time step Δt_{r+1}.

The limiting case of time-dependent propagation law with elastic material behavior is obtained from the preceding algorithm if one sets $J(t,t') = 1/E$ for $t \geq t'$.

An interesting question is how to obtain the solution when the crack propagates according to the classical time-independent law of fracture mechanics (with R-curve) while the material creeps. This situation is approached when $\dot{a} \to 0$ for $K_I < K_I^R(c)$, and $\dot{a} \to \infty$ for $K_I > K_I^R(c)$, i.e., when for $K_I < K_I^R(c)$ the rate $\dot{a}$ is almost 0 and for $K_I > K_I^R(c)$ the rate $\dot{a}$ is extremely large. Such behavior is obtained from Eq. 23 when $n \to \infty$. The foregoing algorithm, however, cannot be expected to converge well for extremely large n values, and it is preferable to obtain the limiting case of time-independent crack propagation law directly. In that case, for a propagating crack we simply have the condition $K_I = K_I^R(c)$, which replaces Eqs. 22-24 while Eqs. 13-21 remain applicable. The values of C_r and C_i in Eqs. 18-21 must now be such that the relation $P_r = b\sqrt{d}\, K_I^R(c_r)/k(\alpha_r)$ be always satisfied, where $c_r = a_r - a_0$, $\alpha_r = a_r/d$. From this relation, the load increment is

$$\Delta P_r = b\sqrt{d}\left(\frac{K_I^R\left(c_{r-1} + \dfrac{\Delta a_r}{2}\right)}{k\left(\alpha_{r-1} + \dfrac{\Delta a_r}{2d}\right)} - \frac{K_I^R(c_{r-1})}{k(\alpha_{r-1})}\right) \tag{25}$$

At the same time, Eq. 18 may be rewritten in the form

$$\Delta u_r = \frac{1}{E_r''}\left[(P_{r-1} + \Delta P_r)C(a_{r-1} + \Delta a_r) - P_{r-1}C_{r-1}\right] + \Delta u_r'' \tag{26}$$

Before stargin the solution of time step Δt_r, the values of $E_r'', \Delta u_r'', P_{r-1}, a_{r-1}, c_{r-1}, \alpha_{r-1}$ are known, and Eqs. 25-26 contain two unknowns, Δa_r and either ΔP_r or Δu_r. If ΔP_r is prescribed, then Δa_r may be solved first from Eq. 25 (e.g., by Newton iterations) and then Δu_r from Eq. 26. If Δu_r is prescribed, then Eqs. 25 and 26 represent two simultaneous nonlinear equations for Δa_r and ΔP_r, and they may again be solved iteratively.

The most important simplification in the preceding solution is the approximation of a crack with a finite fracture process zone and cohesive crack bridging zone by an equivalent sharp crack which supposedly gives about the same overall response of the specimen. This is no doubt adequate for a sufficiently large structure but inadequate for a sufficiently small structure. For smaller structures it is necessary to solve the problem taking at least into account a crack bridging zone of a finite length, which requires postulating a relationship between the crack bridging stress and the crack opening displacement as a material property. This relationship involves both instantaneous response and crack bridging creep. A solution of this type has recently been formulated.

The rate-of-loading effect on fracture has been studied experimentally by the size effect method. The most interesting result [40] is that the effective length of the fracture process zone decreases as the loading rate increases, and thus the response is getting more brittle, closer to LEFM. This is seen in Fig.9 which shows that, for specimens of 3 sizes (1:2:4), for max σ_N-points shift to the right (i.e., toward a higher brittleness β) as the time to reach the peak load increases (tests at constant displacements rates). Measurements are continuing.

4. Closing Remarks

As a final comment on the rate and creep effects, many concrete structures, (for example

dams), develop large cracks over a long period of time. Taking the rate effects in fracture growth as well as material creep (and shrinkage) farther away from the fracture process zone into account is essential for realistic predictions. To present the mathematical groundwork representing perhaps the simplest possible formulation has been one goal of the present workshop contribution. The other goal has been to review a host of recent developments which all exploit in some way a knowledge of the size effect due to fracture This effect itself is a consequence of the nonlocal character of damage in this type of materials.

Acknowledgement

Partial financial support from NSF Center for Science and Technology of Cement-Based Materials at Northwestern University is gratefully acknowledged. Ravindra Gettu of Northwestern University deserves thanks for some expert help in preparation of this manuscript.

References

1. A. Hillerborg, M. Modéer, and P.-E. Petersson, "Analysis of Crack Formation and Crack Growth in Concrete by Means of Fracture Mechanics and Finite Elements," *Cement and Concrete Research* 6(6) (1976), 773-782.

2. Y. S. Jenq and S. P. Shah, "A Fracture Toughness Criterion for Concrete," *Engineering Fracture Mechanics* 21(5) (1985), 1055-1069.

3. S. E. Swartz and T. M. E. Refai, "Influence of Size Effects on Opening Mode Fracture Parameters for Precracked Concrete Beams in Bending," in *Fracture of Concrete and Rock, Proceedings of SEM-RILEM Int. Conf.*, Houston, June 1987, edited by S. P. Shah and S. E. Swartz, Springer-Verlag, NY (1989), 242-254.

4. J. Planas and M. Elices, "Conceptual and Experimental Problems in the Determination of the Fracture Energy of Concrete," in *Fracture Toughness and Fracture Energy, Test Methods for Concrete and Rock*, Preprints of the Proceedings of an Int. Workshop Sendai, Japan, October, 1988, edited by M. Izumi, Tohoku Univ., Sendai, Japan (1988), 1-18.

5. J. Planas and M. Elices, "Size Effect in Concrete Structures: Mathematical Approximations and Experimental Validation," in *Cracking and Damage, Strain Localization and Size Effect*, Proceedings of France-U.S. Workshop, Cachan, France, 1988, edited by J. Mazars and Z. P. Bažant, Elsevier, London (1989), 462-476.

6. H. Horii, Z. Shi, and S.-X. Gong, "Models of fracture process zone in concrete, rock and ceramics," in *Cracking and Damage, Strain Localization and Size Effect*, Proceedings of France-US Workshop, Cachan, France, 1988, edited by J. Mazars and Z. P. Bažant, Elsevier, London (1989), 104-115.

7. M. Elices and J. Planas, "Material Models," in *Fracture Mechanics of Concrete Structures*, RILEM TC90-FMA, edited by L. Elfgren, Chapman and Hall, London, (1989), 16-66.

8. Z. P. Bažant, "Size Effect in Blunt Fracture: Concrete, Rock, Metal," *J. Engng. Mech.*, ASCE, Vol. 110, No. 4 (April 1984), 518-535.

9. Z. P. Bažant and P. A. Pfeiffer, "Determination of Fracture Energy from Size Effect and Brittleness Number," *ACI Mater. J.*, Vol. 84, No. 6, (Nov.-Dec. 1987), pp. 463-480.

10. Z. P. Bažant, "Fracture Energy of Heterogeneous Materials and Similitude," *Preprints, SEM/RILEM Int. Conf. on Fracture of Concrete and Rock* (Houston), edited by S. P. Shah and S. E. Swartz, Soc. for Exp. Mech., 1987; also in *Fracture of Concrete and Rock SEM-RILEM Int. Conf.*, edited by S. P. Shah and S. E. Swartz, Springer-Verlag, New York, (1989), 229-241.

11. Z. P. Bažant and M. T. Kazemi, "Size Effect in Fracture of Ceramics and Its Use for Determining Fracture Energy and Effective Process Zone Length," Report No. 89-6/498s, (1989) ACBM Center, Northwestern University; *J. of American Ceramic Soc.*, in press.

12. Z. P. Bažant, "Mechanics of distributed cracking," *Appl. Mech. Reviews ASME*, 39 (1986), 675-705.

13. R. Gettu, Z. P. Bažant, and M. E. Karr, Fracture Properties and Brittleness of High Strength Concrete, Report No. 89-10/B627f, Center for Advanced Cement-Based Materials, Northwestern University (1989); also *ACI Materials Journal*, in press.

14. Z. P. Bažant and M. T. Kazemi, "Size Effect Tests of Diagonal Shear Fracture," *ACI Materials Journal* (1990), in press.

15. Z. P. Bažant and Hsu-Huei Sun, "Size Effect in Diagonal Shear Failure: Influence of Aggregate Size and Stirrups," *ACI Materials Journal* 84(4) (1987), 259-272.

16. Z. P. Bažant and J. K. Kim, "Size Effect in Shear Failure of Longitudinally Reinforced Beams," *Am. Concrete Institute Journal* 81 (1984), 456-468; Disc. 796 & Closure 83 (1985), 579-583.

17. Z. P. Bažant and Z. Cao, "Size Effect in Shear Failure of Prestressed Concrete Beams," *Am. Concrete Inst. Journal* 83 (1986), 260-268.

18. Z. P. Bažant and Z. Cao, "Size Effect in Punching Shear Failure of Slabs," *ACI Structural Journal* (Am. Concrete Inst.) 84 (1987), 44-53.

19. Z. P. Bažant and S. Sener, "Size Effect in Pullout Tests," *ACI Materials Journal* 85 (1988), 347-351.

20. Z. P. Bažant, S. Sener, and P. C. Prat, "Size Effect Tests of Torsional Failure of Plain and Reinforced Concrete Beams," *Materials and Structures* RILEM, Paris, (1988), 425-430.

21. P. Marti, "Size Effect in Double-Punch Tests on Concrete Cylinders," *ACI Materials Journal* 86(6) (1989), 597-601.

22. R. Eligehausen and J. Ožbolt, "Size Effect in Anchorage Behavior," Proc., ECF8, "Fracture Behavior and Design of Materials and Structures," (1990), 2671-2677.

23. Z. P. Bažant, R. Gettu, and M. T. Kazemi, Identification of Nonlinear Fracture Properties from Size Effect Tests and Structural Analysis Based on Geometry-Dependent R-Curve, Report No. 89-3/498p, Center for Advanced Cement-Based Materials, Northwestern Univ., Evanston, IL., 1989.

24. Z. P. Bažant and M. T. Kazemi, "Size Dependence of Concrete Fracture Energy Determined by RILEM Work-of-Fracture Method," Report No. 89-12/B623s, (1989), NSF Center for Science and Technology of Advanced Cement-Based Materials, Northwestern University, Evanston, IL; also *Int. J. of Fracture*, in press.

25. Z. P. Bažant and Y. Xi, "Statistical Size Effect in Concrete Structures: Nonlocal Theory," Report No. 90-5/616s, (1990), Center for advanced Cement-Based Materials, Northwestern University, Evanston, IL.

26. J. Nakayama, "Direct Measurement of Fracture Energies of Brittle Heterogeneous Materials," *Journal of American Ceramics Society* 48(11) (1965), 583-87.

27. H. G. Tattersall and G. Tappin, "The Work of Fracture and Its Measurement in Metals, Ceramics and Other Materials," *Journal of Material Science* 1(3) (1966), 296-301.

28. A. Hillerborg, "The Theoretical Basis of a Method to Determine the Fracture Energy G_F of Concrete," *Materials and Structures* 18(106) (1986), 291-96.

29. A. Hillerborg, "Results of Three Comparative Test Series for Determining the Fracture Energy G_F of Concrete," *Materials and Structures* 18(107) (1986), 407-13.

30. Z. P. Bažant and F.-B. Lin, "Nonlocal Smeared Cracking Model for Concrete Fracture," *J. of Struct. Eng. ASCE* 114(11) (1988), 2493-2510.

31. Z. P. Bažant and J. Ožbolt, "Nonlocal Microplane Model for Fracture, Damage and Size Effect in Structures," *J. of Eng. Mech. ASCE*, (1990), in press.

32. J. Pijaudier-Cabot, Z. P. Bažant and Y. Berthaud, "Interacting Crack Systems in Particulate or Fiber-Reinforced Composites," Proc., 6th Int. Conf. on Numerical Methods on Fracture Mechanics (1990), held in Freiburg, West Germany, April 1990.

33. H. Gao and J. R. Rice, "A First order Perturbation Analysis on Crack Trapping by Arrays of Obstacles," Report Division of Appl. Sciences, Harvard Univ., Cambridge MA, Nov. 1988.

34. T. Mori, K. Saito and T. Mura, "An Inclusion Model for Crack Arrest in a Composite Reinforced by Sliding Fibers," *Mech. of Materials* Vol. 7 (1988), 49-58.

35. P. C. Paris, M. P. Gomez, and W. E. Anderson, "A Rational Analytic Theory of Fatigue," *The Trend in Engineering* 13(1) (Jan. 1961).

36. P. C. Paris and F. Erdogan, "A Critical Analysis of Propagation Laws," *Transactions of ASME, J. of Basic Engrg.* 85 (1963), 528-534.

37. S. E. Swartz and C. G. Go, "Validity of Compliance Calibration to Cracked Beams in Bonding," J. of Experimental Mech. 24(2) (June 1984), 129-134.

38. Z. P. Bažant and K. Xu, "Size Effect in Fatigue Fracture of Concrete," Report No. 89-12/623s, (1989), ACBM Center, Northwestern University; submitted to *ACI Mat. J.*.

39. Z. P. Bažant and P. C. Prat, "Effect of Temperature and humidity on fracture energy of concrete," ***ACI Materials J.* 84 (July 1988), 262-271.**

40. Z. P. Bažant and R. Gettu, "Determination of Nonlinear Fracture Characteristics and Time Dependence from Size Effect," in *Fracture of Concrete and Rock: Recent Developments*, Proc. Int. Conf. in Cardiff, UK, edited by S. P. Shah, S. E. Swartz and B. Barr, Elsevier Applied Science, London, (1989), 549-565.

41. Z. P. Bažant, Editor (1988), "Mathematical Modeling of Creep and Shrinkage of Concrete," John Wiley and Sons, Chichester and New York.

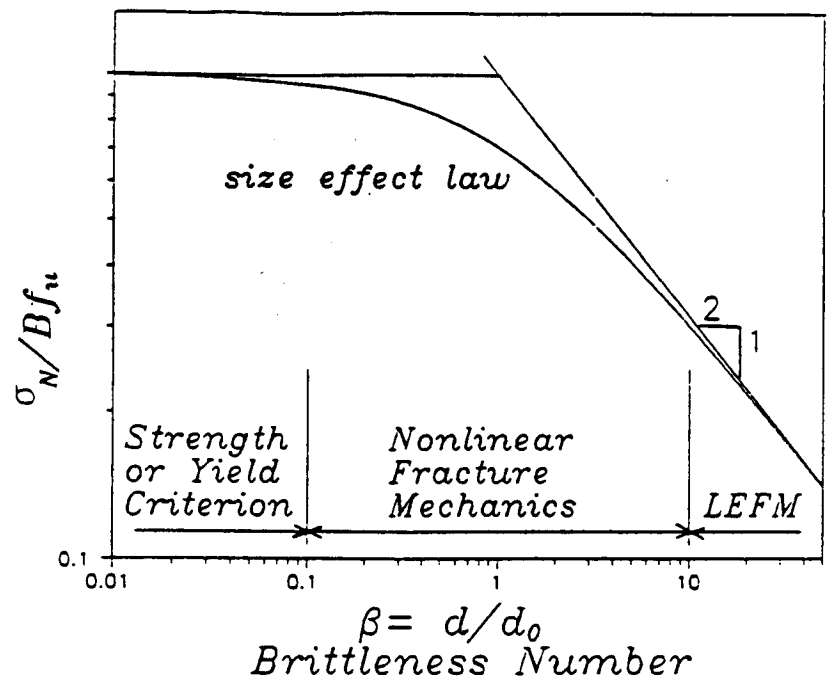

Fig.1. Size effect law for quasi-brittle structures.

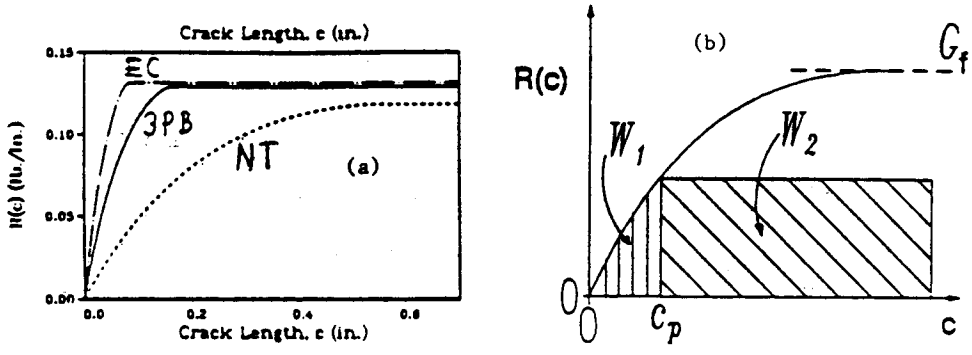

Fig.2. R-curves and effect of size on fracture energy, along with an idealized picture of the evolution and movement of fracture process zone.

(c)

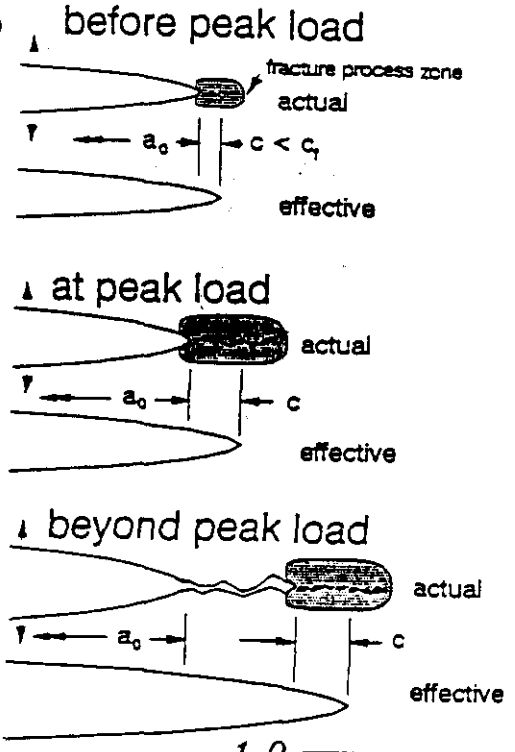

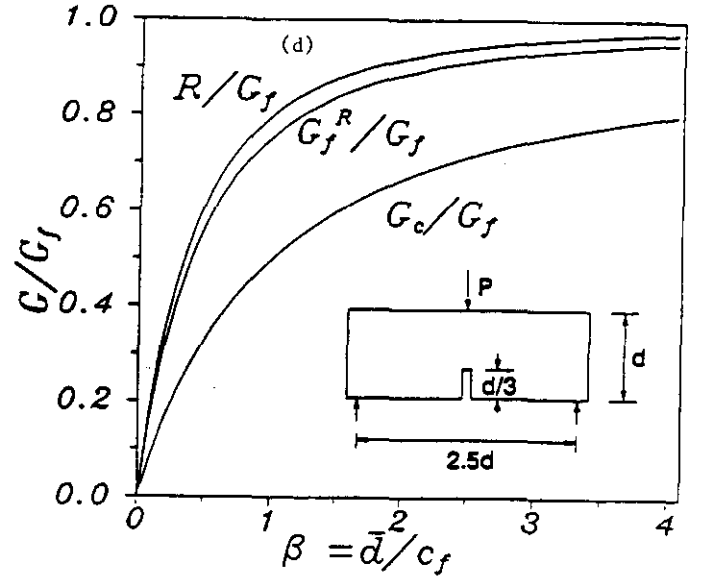

Fig. 2 continued

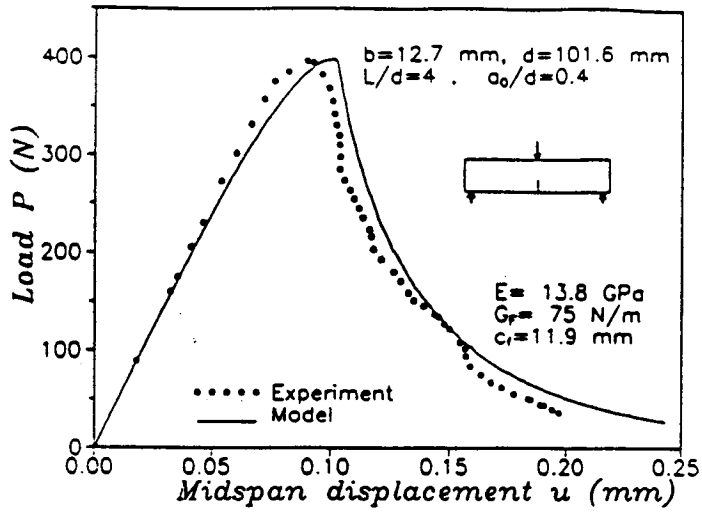

Fig.3. Prediction of the load-deflection curve from measured maximum loads of rock fracture specimens of different sizes, in comparison with the load- deflection curve measured by Bažant, Gettu, and Kazemi [23].

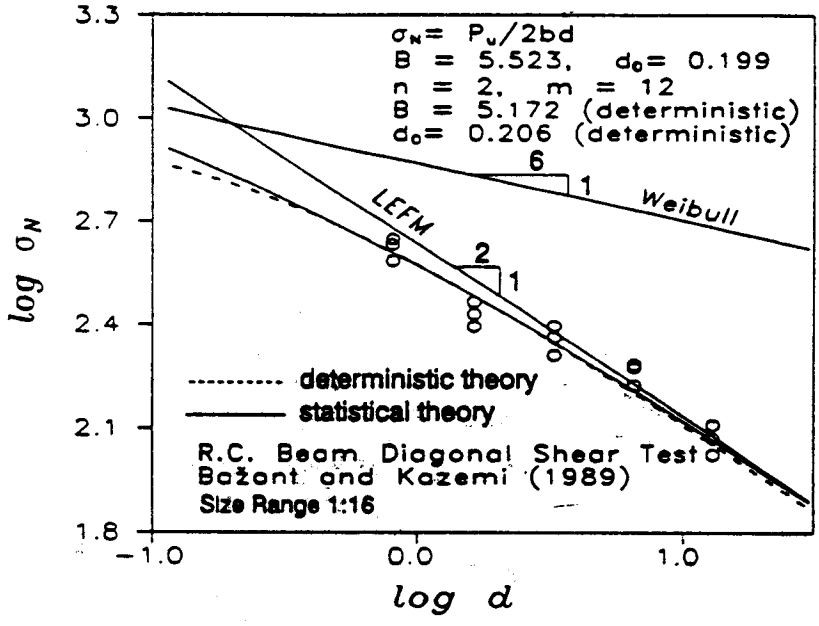

Fig.4. Statistical generalization of the size effect law.

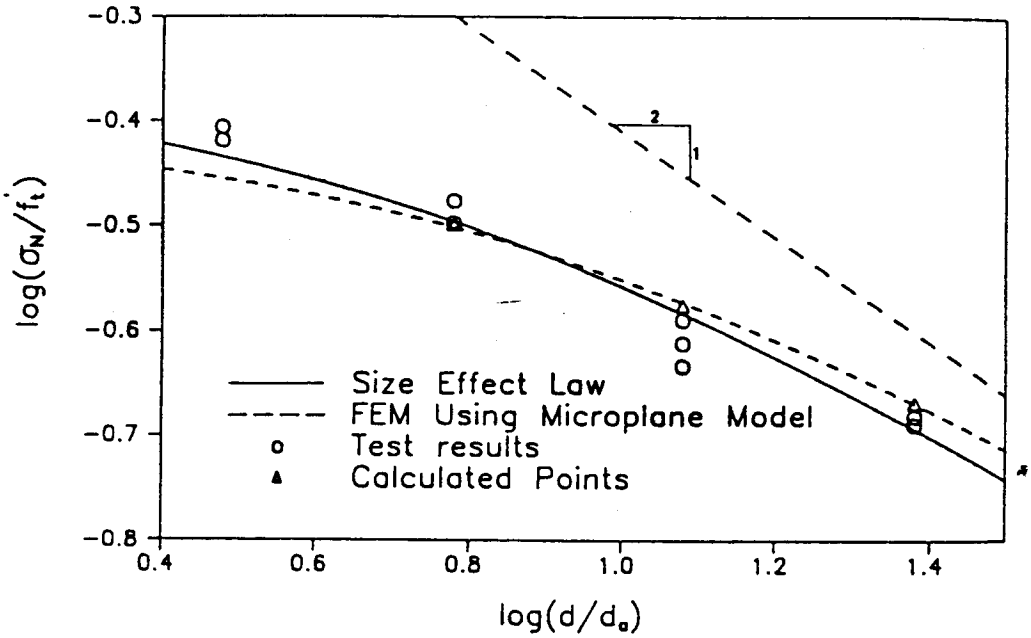

Fig.5. Nominal strengths of fracture specimens of different sizes calculated by a finite element program based on nonlocal microplane material model, compared with the size effect law and with experimental measurements of Bažant and Pfeiffer [9].

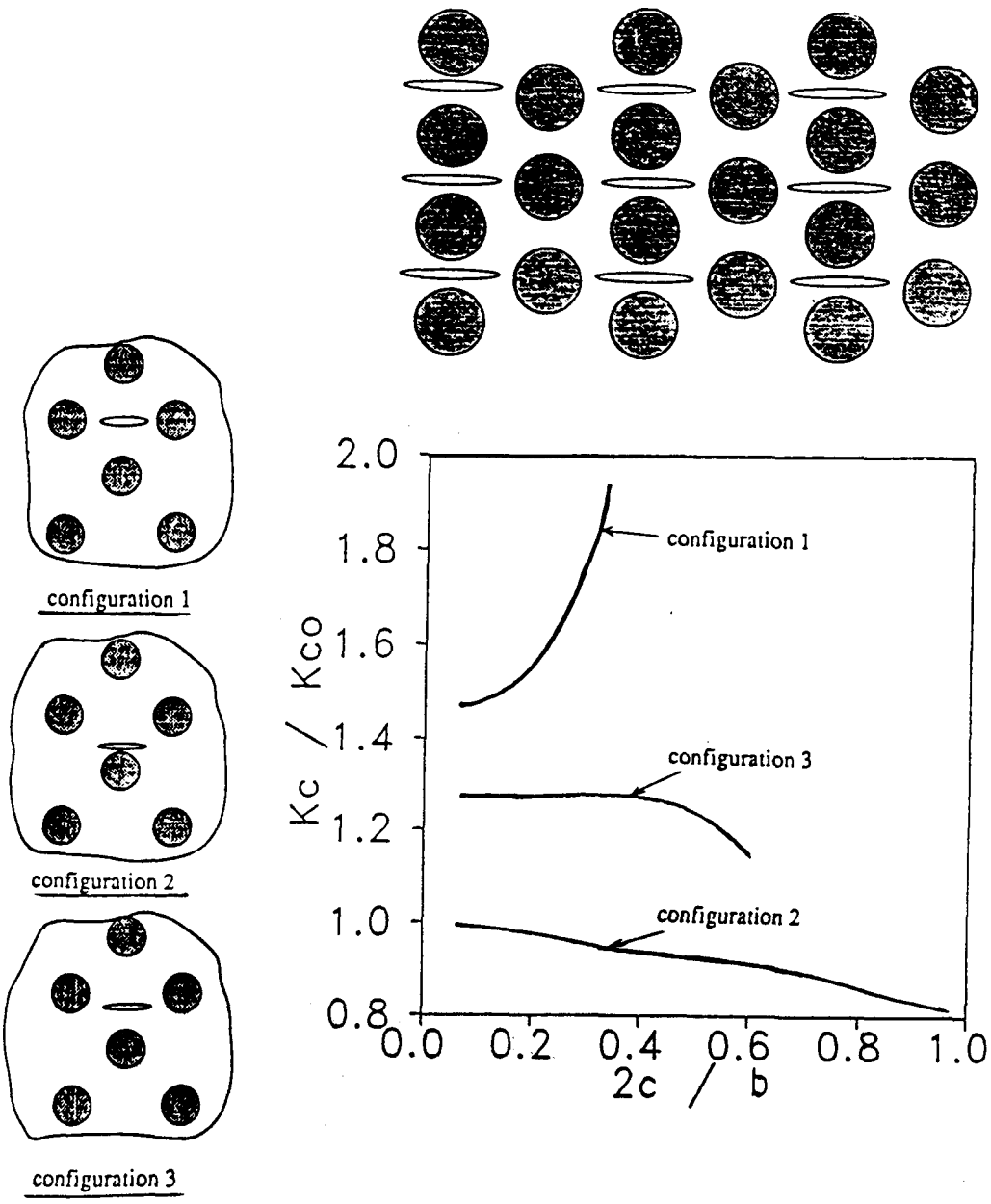

Fig.6. Approximation of fracture process zone by an elastic matrix with microcracks and inclusions, and apparent R-curves for the microcracks calculated by Pijaudier Cabot, Bažant and Berthaud [32].

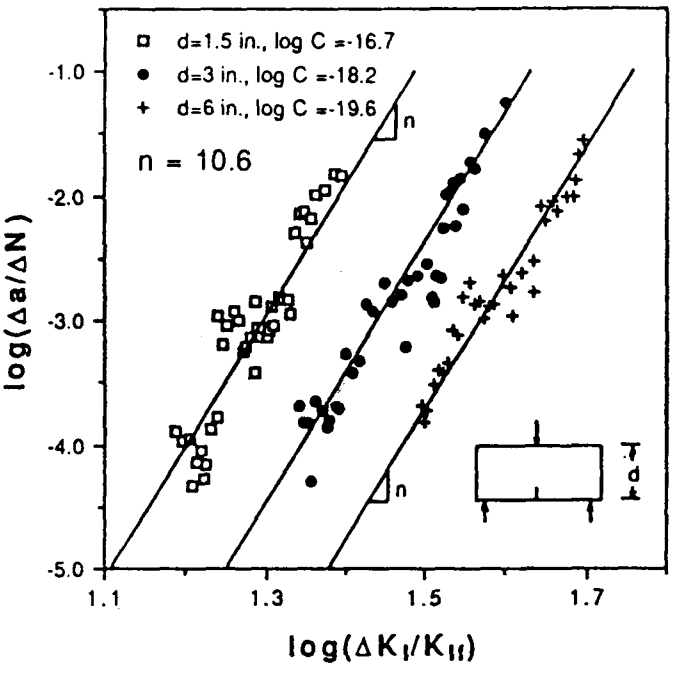

Fig.7. Test results of Bažant and Xu [38] on fatigue fracture of concrete specimens of three different sizes and their comparison with size-adjusted Paris law.

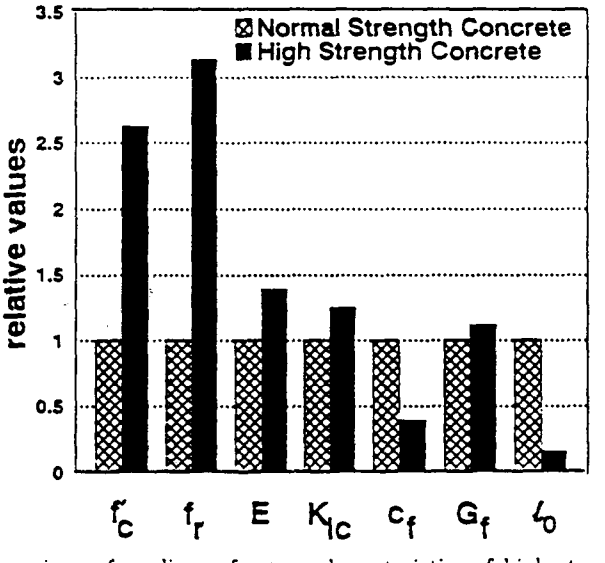

Fig.8. Comparison of nonlinear fracture characteristics of high strength concrete and normal concrete [13].

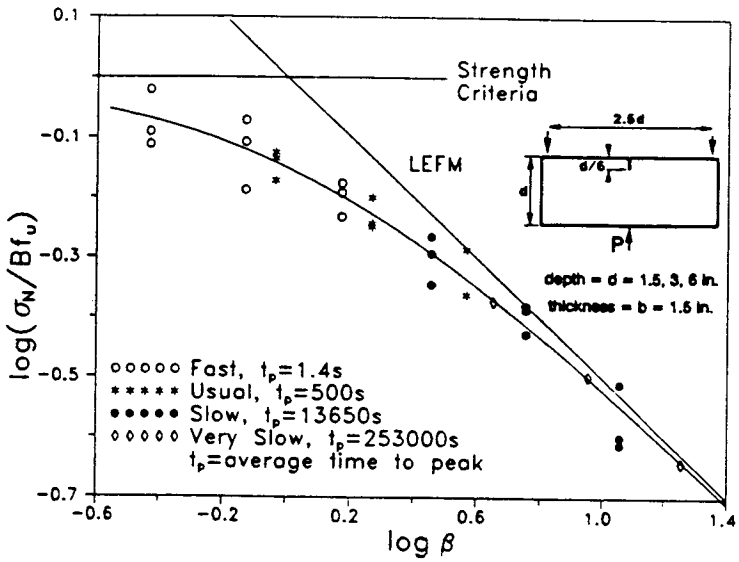

Fig.9. Size effect on nominal strengths at different loading rates, reported by Bažant and Gettu [40].